



## The Activity of Gamma Irradiated Poly (Thiourea–Formaldehyde) Resin against Aquatic Microbes and Cytotoxic Activity

Ahmed Awadallah-F<sup>1</sup>, Ahmed M. Azzam<sup>2\*</sup>, Bayaomy B. Mostafa<sup>2</sup>  
Ahmad S. Kodous<sup>3</sup>, Magd M. Badr<sup>4</sup>

- 1- Radiation Research of Polymer Department, Industrial Irradiation Division, National Center for Radiation Research and Technology (NCRRT), Egyptian Atomic Authority (EAEA), Cairo, Egypt.
- 2- Environmental Research Department, Theodor Bilharz Research Institute (TBRI), Egypt.
- 3- Radiation Biology Department, National Center for Radiation Research and Technology (NCRRT), Egyptian Atomic Energy Authority (EAEA), Cairo, Egypt.
- 4- Polymer Laboratory, Petrochemical Division, Egyptian Petroleum Research Institute (EPRI), Nasr City, Cairo, Egypt.

\*Corresponding authors: [ah.azzam@tbri.gov.eg](mailto:ah.azzam@tbri.gov.eg)

### ARTICLE INFO

#### Article History:

Received: Oct. 25, 2022

Accepted: Nov. 21, 2022

Online: Dec. 9, 2022

#### Keywords:

Gamma rays,  
Poly (thiourea–  
formaldehyde)  
resin,  
Antimicrobial,  
Cytotoxic,  
Wastewater

### ABSTRACT

Poly (thiourea–formaldehyde) resin (PTUFR) is synthesized by gamma rays. Fourier transform infrared (FTIR), <sup>1</sup>H-NMR and <sup>13</sup>C-NMR spectroscopy, transmission electron microscopy (TEM), and gel permeation chromatography (GPC) were the techniques used to characterize PTUFR. The results confirmed the formation of PTUFR. The antimicrobial activity of PTUFR was tested against the most resistant isolated aquatic microbes Gram-positive bacteria (*Bacillus subtilis*), Gram-negative bacteria (*Pseudomonas aeruginosa*), and fungi (*Candida albicans*). Through the interaction with internal cellular components and cell membranes, PTUFR showed potential for bio-application in inactivating microbial cells by killing them. The two cell death mechanisms of the reactions of PTUFR with the proteins of the cell wall led to reduced permeability, as well as reactive oxygen species (ROS) with high release rates from PTUFR, which in a row caused damage to DNA and cellular components. Furthermore, the cytotoxicity of PTUFR against human breast cancer MCF-7 and HepG2 liver cancer cells was studied. The cytotoxicity of PTUFR resulted in the inhibition of cell growth on the lines of the cancer cells. [Z1] The exposure of MCF-7 and HepG2 cancer cells to PTUFR for 48h displayed a potential apoptotic activity by significant upregulation of p53 gene expression and cytotoxic activity by downregulation of Bcl-2 gene expression. These results may also contribute to an unconventional strategy for environmental and medical applications, such as safe wastewater disinfection and cytotoxic activity.

### INTRODUCTION

The synthesis of formaldehyde-based polymers containing the donor groups of nitrogen, oxygen, sulphur, and phosphorus has been used motivated by applied research, including composite materials, modeling compounds, adhesive, wood industry and coatings (Xu *et al.*, 2022). Many duties were noted for controlling the organic polymers disadvantages of heating breakdown in air and microorganism infection by using metal ions additives in the polymer composite and nanocomposites (Wang *et al.*, 2022). Groups like –NH<sub>2</sub>, –COOH, –OH and –C=O in the organic

polymers are called donor groups that interact with transition metal ions to form thermally stable coordination polymers. This kind of material provides both high flexibility and thermal stability. The existence of organic parts and inorganic fractions in the same polymeric backbone combine these properties together (**Chen *et al.*, 2021; Xue *et al.*, 2022**). Coordinated polymers were widely synthesized using thiourea and its derivatives such as bidentate ligands due to the special chemical structure of thiourea. These properties of the polymeric complexes formed qualify the material to be used in a wide range of applications (**Barzaga *et al.*, 2021**). These applications include catalysts, semiconductors, and thermal insulator coatings in aircraft and space industries, among others (**Liu *et al.*, 2022**). The chemical nature of the moiety attached to the C=S carbon atom featured of thiourea shows significant antibacterial and antifungal activities and possesses medicinal properties (**Li *et al.*, 2022**). It is also used as biocidal coatings and is widely applied to decrease the growth of microorganism on surfaces including antifouling paints in marine uses (**Uçak & Aydın, 2022**). The chemical composition of thiourea containing bidentate functional nature of sulfur and nitrogen as donor groups promotes us to use thiourea-formaldehyde resins (TUFRS) for coordinating polymer synthesis. A considerable interest has been drawn to compounds containing nitrogen and sulfur in the potential biological activity (**Benis *et al.*, 2022**).

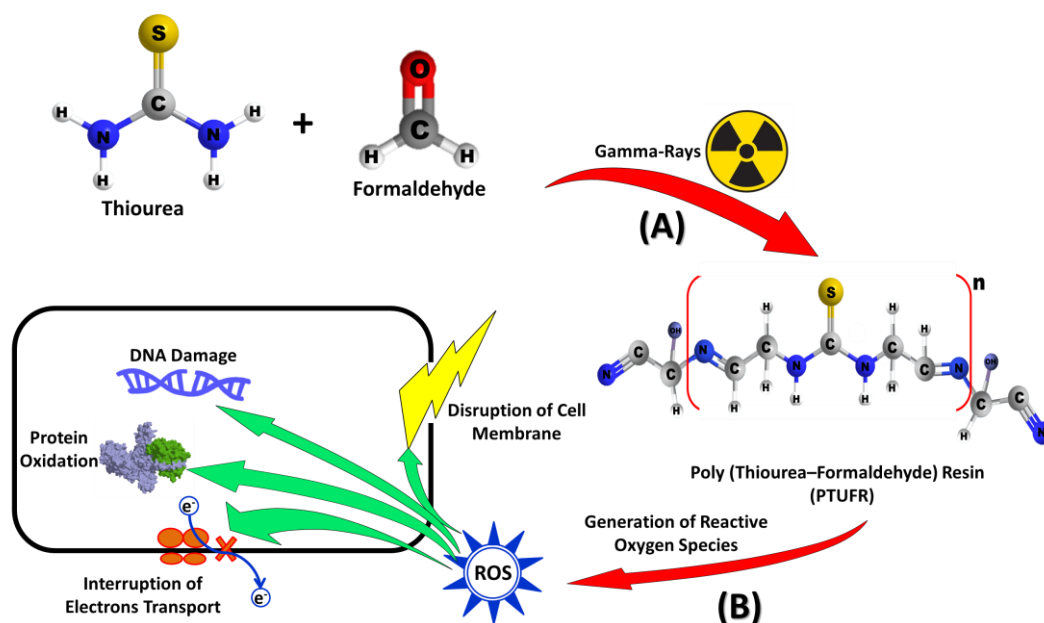
The desired properties of limited residual toxicity do not permeate through skin; the chemical stability, non-volatile, and long-term polymer material recently increased the demand on the antimicrobial polymers. The efficiency, quality, fungal, and bacterial activities of the antimicrobial polymer are based on the functional groups and molecular weight. The chemical composition has to be considered well during synthesis through deciding the polymer application. The antimicrobial polymers have a variety of applications, viz. surgical instruments, coatings, textile, adhesives, agriculture and metallurgy. The antimicrobial polymers reduce the leaching out of bioactive substances (**Ojogbo *et al.*, 2020**). To overcome this related problem, various researchers are synthesizing high molecular weight antibacterial agent materials, which can maintain ecological balance and are naturally eco-friendly (**Zhong *et al.*, 2020**). Thiourea has potent antifungal activity similar to that found in the common antifungal drug ketoconazole. In addition, it has insecticidal and antibacterial properties (**Kavyasri *et al.*, 2022**).

Cancer is one of the most serious health problems worldwide. By 2030, cancer cases are expected to reach 20 to 30 million new cases, of which 13 to 17 million deaths by cancer are predicted. The cancer cells are characterized with the preservation of proliferative signaling, allowing replication, angiogenesis induction, resistance to cell death, the avoidance of growth suppressors, invasion and metastasis activation, immune depletion avoidance, and energy metabolism rewiring. Potential cancers are persistent and widespread throughout the body caused by genomic mutations due to endogenous and/or exogenous factors affecting the regulatory functions of cells. Cancer most often occurs in humans due to genetic factors. Lifestyle factors such as tobacco chewing and smoking; certain types of infections

and exposure to various chemicals and radiation (**Lewandowska *et al.*, 2019**; **Ward *et al.*, 2021**) are associated with cancer.

Hence, medicinal research society considered thiourea as one of the active areas of research. Efforts are currently focused in order to have better new therapeutic agents. **Arafa *et al.* (2022)** detected an efficient anticancer activity of the thiourea polymer against different cancer cell lines, including mediated multidrug-resistant cancer cell lines. Furthermore, it showed a potent anticancer activity against MCF-7, HCT116, and A549 cancer cell lines. The production of reactive sulfur species (RSS), reactive oxygen species (ROS), and reactive nitrogen species (RNS) was increased in a concentration-dependent manner in polymers based thiourea treated MCF-7, HCT116 and A549 cells. Moreover, thiourea polymer led to apoptosis by DNA damage in cancer cells by inserting directly into the DNA or the overproduction of ROS and/or RNS, which activated caspase activity. Hence, thiourea polymer is a promising anticancer therapeutic agent (**Arafa *et al.*, 2022**). Previous studies postulated that, the overproduction of ROS leads to DNA damage, proteins, and organelles destruction, hence the induction of apoptosis to display a cytotoxic effect is effective. For this reason, the induction of oxidative stress using anticancer drugs is a valuable therapeutic strategy in order to destroy the cancer cells. Likewise, NO and RNS overproduction causes nitrosative stress, leading to programmed cell death. Moreover, it was reported that, ROS and RNS overproduction induces mitochondrial (intrinsic) apoptotic pathway in cancer cells (**Bai *et al.*, 2021**). **Hormati *et al.* (2021)** noticed that 1, 3- phenyl bis- thiourea induces prometaphase mitotic, arresting prolonged to apoptosis and inhibiting tubulin polymerization. It was found that, 1, 3-phenyl bis-thiourea antagonizes drug resistance by binding to  $\beta$ -tubulin mutation and P-glycoprotein overexpression. Thiourea derivatives have a potent anticancer therapeutic agent.

The present work focused on gamma irradiation synthesis, physicochemical characterization, antimicrobial, and the cytotoxic evaluations of poly (thiourea-formaldehyde) resin (PTUFR). The characterization techniques used were: fourier transform infra-red (FTIR), proton nuclear magnetic resonance ( $^1\text{H-NMR}$ ) spectroscopy and carbon-13 nuclear magnetic resonance ( $^{13}\text{C-NMR}$ ) spectroscopy, transmission electron microscopy (TEM), and gel permeation chromatography (GPC). The microorganisms used in this work were: *Bacillus subtilis* Gram-positive, *Pseudomonas aeruginosa* Gram-negative, and *Candida albicans* fungi. Moreover, the PTUFR could be used as cytotoxic agent against human breast cancer cells MCF-7 and HepG2 liver cancer cells, as shown in Scheme "1".



**Scheme 1.** A) The proposed reaction mechanism of poly (thiourea-formaldehyde) resin formation induced by  $\gamma$ -rays, and B) Poly (thiourea-formaldehyde) resin formation induced by  $\gamma$ -rays and the effects of PTUFR on the cell.

## MATERIALS AND METHODS

### Materials

Formaldehyde (37 % aqueous solution) and thiourea (purity  $\geq 99.0\%$ ) were purchased from Sigma-Aldrich (Germany). Ampicillin, gentamicin, and amphotericin-B antibiotics were supplied from Bio-Rad, France. All reagents were analytically pure, thus were not further purified. All the microorganisms were isolated from water and then identified and classified in Environmental Research Department, Theodor Bilharz Research Institute, Egypt (TBRI). The cell lines (MCF-7 and HepG2) were provided by the laboratory of NCRRT.

### Experimental section

#### *Synthesis of poly (thiourea–formaldehyde) resin (PTUFR)*

The poly (thiourea–formaldehyde) copolymer resin was polymerized from thiourea and formaldehyde monomers, as shown in Scheme (1). Thioureas (15.2g) dissolved in 40mL methanol (50 % aqueous solution) were magnetically stirred in a 250mL flask at room temperature until being completely dissolved. Fifteen mL of a 37 % aqueous solution of formaldehyde was added to aqueous solution of thiourea. The mixture was magnetically stirred for 2 hours at room temperature to obtain the complete dissolution (Kanwal *et al.*, 2020). Then, the mixture was exposed to gamma irradiation at dose 5kGy of dose rate 0.9kGy/ h. The outcome product was washed by distilled water and methanol three times for each solvent to clean it from unreacted thiourea and formaldehyde. Moreover, the yield of product was 70%.

### **Characterization of PTUFR**

The infrared spectra were investigated using Fourier transform infra-red (FTIR) spectrophotometer, Perkin Elmer, USA, with range of 4000–400  $\text{cm}^{-1}$ . Proton nuclear magnetic resonance ( $^1\text{H-NMR}$ ) spectroscopy and carbon-13 nuclear magnetic resonance ( $^{13}\text{C-NMR}$ ) spectroscopy were measured using 300 MHz model (Bruker AMX-R300). The  $^{13}\text{C-NMR}$  spectra were obtained with 9.5 seconds pulse width (30) and a pulse delay of 4 seconds. Transmission electron microscopy (EM 208S Philips, Netherlands) operated at an acceleration voltage of 80 kV was utilized in the current study. Gel-permeation chromatography (GPC) (refractive index detector, empower TM2 chromatography data software flow 1mL/ min, mobile phase THF) was utilized to find out the average molecular weight.

### **Antimicrobial activity assay**

#### **Agar well diffusion method**

The microbicidal activity of PTUFR was determined using agar well diffusion method and observed against the most prevalent bacterial strains in water environment Gram-positive (*Bacillus subtilis*), Gram-negative (*Pseudomonas aeruginosa*), and fungi (*Candida albicans*), previously isolated and identified in TBRI from wastewater using conventional microbiological techniques. Each species was cultured on specific media and temperature on shaker incubator (180 rpm) for 24 hours. Six mm wells were punched into plates (Nutrient agar for bacteria and Sabouraud Dextrose agar (SDA) for fungi). Using a micropipette, 100 $\mu\text{L}$  PTUFR water suspensions (10mg/ mL) was placed in wells in used plates. After the incubation time (24 hours), the different levels of zone of inhibition were measured. Triplicate plates were used for each concentration and organism (Azzam *et al.*, 2022).

#### **Water viable microbial counts (VMCs) assay**

Viable microbial counts (VBCs) assay evaluated each microbe species in water at different times after treating water with 10mg/ mL of PTUFR, then the count of surviving microbes in water *B. subtilis*, and *P. aeruginosa*, and *C. albicans* was determined by the plate count technique (Azzam *et al.*, 2019). The reduction percentage of VMCs was calculated after treating with PTUFR according to the succeeding formula:

$$\text{VMCs Reduction \%} = \frac{\text{Viable count at time 0} - \text{Viable count at time } x}{\text{Viable count at time 0}} \times 100 \quad \dots\dots\dots (1)$$

where, time<sup>0</sup> is the time before adding PTUFR, and time<sup>x</sup> is the contact time between contaminated water with microbe and PTUFR resin.

#### **Bacterial minimal inhibitory concentration (MIC)**

The MIC of bacterial strains *B. subtilis* and *P. aeruginosa* was assayed using serial dilutions for PTUFR at concentrations from 1.0- 10mg/ mL; the bacterial inoculums of 0.5 McFarland turbidity. The MIC was tested in triple for each bacterial species (Azzam *et al.*, 2019).

**Minimal fungicidal concentration (MFC)**

The MFC of PTUFR was tested for *C. albicans* fungi culture onto Sabouraud Dextrose Agar plates and during 3 days at 28°C for detecting the minimum concentration of PTUFR inhibiting the fungal growth on growth media (Dylağ *et al.*, 2019).

**Morphological characterization of treated bacteria and fungi**

Bacterial and fungal cells exposed to PTUFR and control ones were examined by transmission electron microscope (EM 208S Philips, Netherlands). The standard protocol was used for preparing samples. Slices of 60nm thickness were made using a diamond knife. The slices were put on copper grids and stained with uranyl acetate. Morphological features of cells were studied using TEM at 80 kV for studying the biocidal action of PTUFR (Azzam *et al.*, 2022).

**MTT Cytotoxicity assay of PTUFR**

A reacting *in vitro* assay for assessing cell reproduction using the easiest test utilizes 3-[4,5-dimethylthiazol-2-yl]-2,5-diphenyl tetrazolium bromide (MTT assay), as standard protocol (Abel & Baird, 2018). MCF-7 and HepG2 cancer cells were cultured with PTUFR (50, 25, 12.5, 6.25 and 3.125µg/ mL) ratio of 1:1 and incubated for 48 hours in 5% CO<sub>2</sub> incubator. The percent of viable cells was calculated according to the following equation:

$$\text{Viable Cell \%} = \frac{\text{Sample Absorbance} - \text{Blank Absorbance}}{\text{Control Absorbance} - \text{Blank Absorbance}} \times 100 \quad \dots \quad (2)$$

**Real time PCR for P53 and Bcl-2 gene expressions**

To reveal p53 and Bcl-2 gene expression, applied biosystems 7500 was used (Triplicate) as a standard method (Badr *et al.*, 2020). The code levels of p53 and Bcl-2 mRNAs were detected by Ct. to assess mRNA expression. To normalize the proportional profusion of p53, and Bcl-2 mRNAs, Taqman mRNA assays for glyceraldehyde-3-phosphate dehydrogenase protein were used.

**RESULTS AND DISCUSSION****Characterization of PTUFR**

Fig. (1A) shows the FTIR spectrum of formaldehyde with bands at 3310, 2922 and 2841 cm<sup>-1</sup> for OH of H<sub>2</sub>O, and symmetric and asymmetric –CH. The peak at 1640 cm<sup>-1</sup> for –C=O for aldehyde. The spectrum of pure thiourea peaks is the C=S vibration appears at 730 cm<sup>-1</sup>, coupled C–N asymmetric stretching, C–N stretching and N–H bending at 1470, 1073 and 1604 cm<sup>-1</sup>, and symmetric and asymmetric N–H stretching at 3143 and 3280 cm<sup>-1</sup>, respectively. The characteristic peaks of poly(thiourea-formaldehyde) resin (PTUFR) appear coupled C–N asymmetric stretching, and C–N stretching at 1465, and 1063 cm<sup>-1</sup>, symmetric and asymmetric N–H stretching at 3170 and 3285 cm<sup>-1</sup>, respectively. C=S appears at 1152 cm<sup>-1</sup>, N–C=S appears at 1640 cm<sup>-1</sup>, C=NH appears at 1530 cm<sup>-1</sup>, C=S vibration appears at 717 cm<sup>-1</sup>. The peak is at 2060 cm<sup>-1</sup> refers to –SCN. The peaks that papers in the range 635-602 cm<sup>-1</sup>, may be attributed to C–S stretching vibrations (Ganesan *et al.*, 2022).

Further, from Table "1" it can be observed that the  $M_w$  of PTUFR is around 35 kDa according to the GPC results. Additionally, from the elemental analysis results, the molar percentage of N (29.2%), S (33.4 %), C (32.1%), and H (5.3%) in the PTUFR (Li *et al.*, 2020).

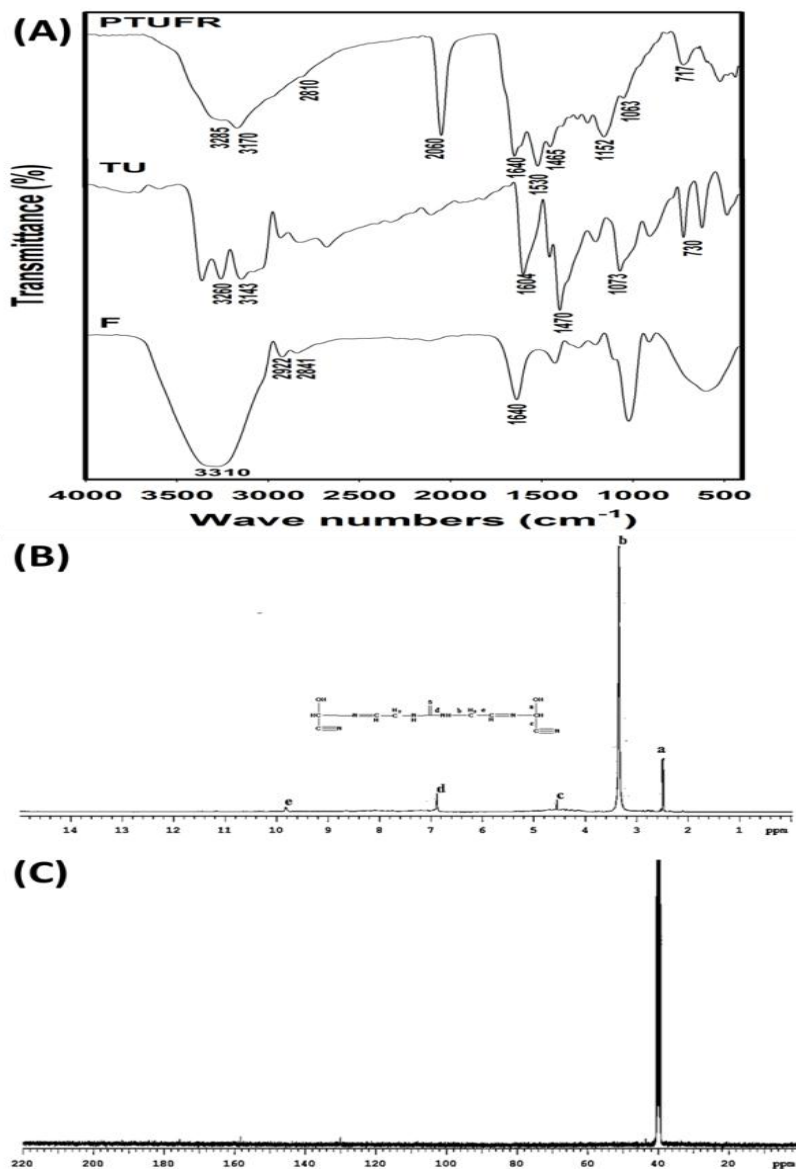


**Fig. 1.** A) FTIR, B) <sup>1</sup>H NMR spectrum, and C) <sup>13</sup>C NMR spectrum of poly (thiourea-formaldehyde) resin (PTUFR).

**Table 1.** GPC and CHNS analysis of PTUFR.

GPC PTUFR			
Retention time	$M_n$	$M_w$	Polydispersity
23.513	23644	35382	1.49
CHNS analysis			
N (%)	S (%)	C (%)	H (%)
29.2	33.4	32.1	5.3



The  $^1\text{H}$ -NMR spectrum of PTUFR is depicted in Fig. 1B. The spectrum of the resin exposed a signal at 6.80 ppm for the NH protons of the thioamide group, which had actually shifted downfield from its original position at 7.25 ppm due to the intramolecular and intermolecular hydrogen bonding between the C and NH of the PTUFR and the S=O groups of the solvent. The signal at 2.6 ppm referred to proton of OH (OH–CH), 3.5 ppm referred to CH (N–CH<sub>2</sub>-), 4.5 ppm referred to CH (=N–CHOH –C≡N), 6.9 ppm (CH=N), and 9.8 ppm referred to residue of (formaldehyde) (Mane et al., 2009).

The  $^{13}\text{C}$ -NMR spectrum of the PTUFR is shown in Fig. 1C. The  $^{13}\text{C}$ -NMR spectra of PTUFR showed a peak at around 40 ppm. According to published information, this chemical shift (around 40 ppm) is referred to the carbon of methylene linkages. The chemical shift at 130 ppm referred to thioamide group. The peak at 158 ppm is referred to the carbons of carbonyl group of formaldehyde residues (Sayed et al., 2018).

### Antimicrobial activity of PTUFR

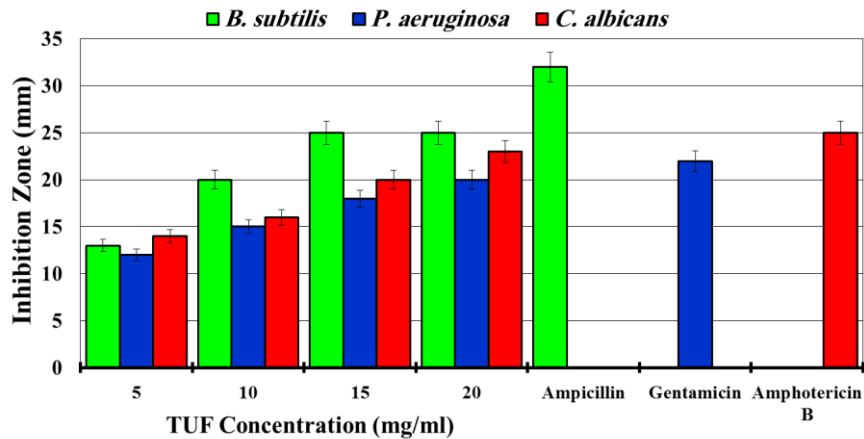
#### Inhibition zone (IZ) assay

Fig. 2 shows the inhibition zones of different types of PTUFR against the tested waterborne bacteria. The inhibition zones showed that PTUFR have variable micobicial activity for bacteria and fungi. The highest inhibition zones were recorded with PTUFR concentration 15 mg/mL, were represented 25 and 18 mm against *B. subtilis* and *P. aeruginosa*, and at 20 mg/mL for *C. albicans* by 23 mm, respectively. However, by increasing or decreasing Gamma ray dose inhibition zones decreased, as shown in Fig. "2". Gram-positive bacteria and *C. albicans* were more sensitive toward PTUFR than Gram-negative one. This consequence is due to the difference in the susceptibility of the two types of microbes to PTUFR antibacterial agent due to the variation in cell wall building. Where the cell wall of the positive type is simpler than the negative one, so the cell membrane of the positive one can be damaged more easily than the negative one (El-Liethy et al., 2018).

#### Water viable microbial counts (VMCs) assay

As shown in Fig. "3" the antimicrobial killer-time assay for viable microbial counts in water showed that the VMCs of *B. subtilis* and *P. aeruginosa* bacteria and *C. albicans* fungi treated with 10 mg/ mL of PTUFR resin at zero contact time were and 75, 68, and 71 × 10<sup>4</sup> cfu/mL, respectively, whereas VMCs recorded 35, 36, and 32 × 10<sup>4</sup> cfu/mL with reducing percent of 53%, 47%, and 55%, respectively, after 1.0 hour of exposure. By increasing exposure time inhibition percent increase, where after 9 hours were 97%, 85%, and 100%, respectively. However, the reduction reached 100%, 96%, and 100% after 12 hours. Moreover, all microbial cells were competently inhibited at 18 hours. The interaction between microbial cells and PTUFF was sufficient to deactivate all microbial cells (El-Liethy et al., 2018).





**Fig. 2.** Inhibition zones of tested microorganisms and antibiotics treated with different PTUFR concentrations.

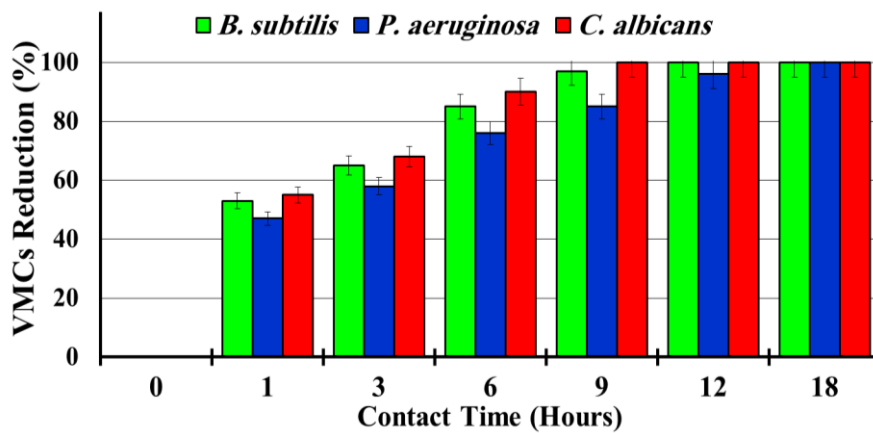


**Fig. 3.** Viable microbial counts (VMCs) reduction percent of treated microorganisms in water against PTUFR concentrations.

### Minimal Inhibitory Concentrations

The MICs of PTUFR were estimated against tested bacterial strains and fungi. The resulted values of MICs for PTUFR were 0.42, 0.67, and 0.50 mg/mL with *B. subtilis*, *P. aeruginosa*, and *C. albicans*, respectively. Consequently, PTUFR could show a highly promising antimicrobial agent that can be used in wastewater treatment for waterborne microbes' inhibition that contaminated our water sources (El-Liethy *et al.*, 2018).

### Morphological characterization of bacteria and fungi

Figure "4" showed the different effects of PTUFR on both bacterial and fungal cells. The Gram-positive (*B. subtilis*), Gram-negative (*P. aeruginosa*) bacteria and fungus (*C. albicans*) were treated with PTUFR and the morphological futures were determined by TEM before and after exposure. TEM images confirmed the presence of disorders on microbial cells included damage of cell wall, lysis of interior cell contents, such as DNA, protein oxidation, and interruption of electrons transport leading to microbial cell death, as shown in Fig. "4" and Scheme "1" (Azzam *et al.*, 2022).

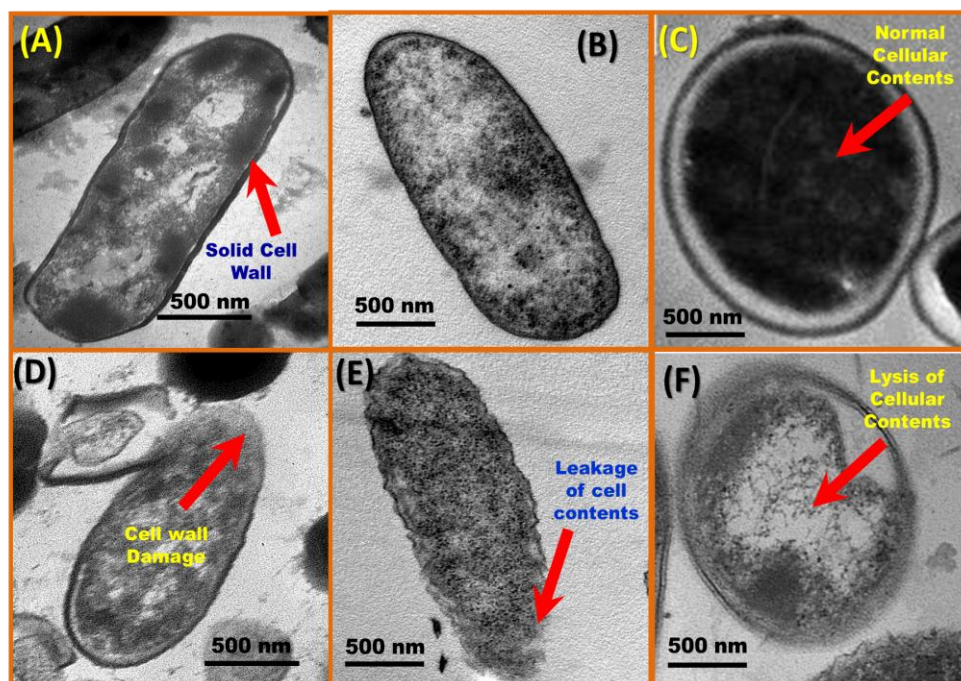


**Fig. 4.** TEM images of *B. subtilis*, *P. aeruginosa*, and *C. albicans* control (A–C) and treated with PTUFR (D–F).

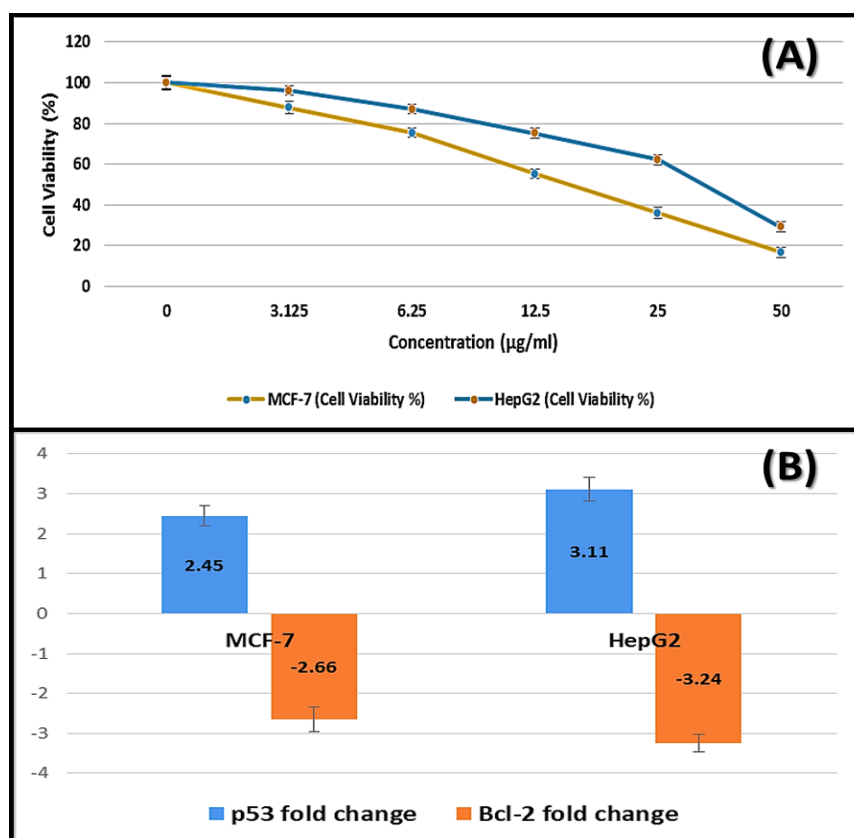


**Fig. 5.** A) Cell viability in MCF-7 and HepG2 cancer cells incubated with different PTUFR concentrations. B) The gene expression of P53 and Bcl-2, as fold gene expression in MCF-7 and HepG2 post 48 h incubation with PTUFR.

### Cell inhibition performance of PTUFR using MTT

Figure "5A" showed the results of the cytotoxic effect of PTUFR against MCF-7 and HepG2 cancer cell lines. The cell viability was observed in previous cancer cell lines incubated with different concentrations of PTUFR using MTT test. Viable cancer cells incubated in RPMI complete media were considered as a positive control (100 % viability). The greater inhibitory concentration value for PTUFR was at 50  $\mu\text{g/mL}$  in MCF-7 and HepG2 exhibited 83.32 and 70.87 %, respectively after 48 hours of incubation than other concentrations of 25, 12.5, 6.25, and 3.125  $\mu\text{g/mL}$  which exhibited 64.17, 44.87, 24.52, and 12.14 % MCF-7 cell inhibition, respectively, and 37.76, 24.81, 13.14, and 3.94 % HepG2 cell inhibition, respectively. The  $\text{IC}_{50}$  of PTUFR in MCF-7 and HepG2 was 14.45 and 25.08  $\mu\text{g/mL}$  respectively. The results suggested PTUFR perform further experiments (Arafa *et al.*, 2022).

### The effect of PTUFR on gene expression of P53 and Bcl-2

The gene expressions of Bcl-2 in MCF-7 and HepG2 cancer cells were decreased after incubation for 48 hours with 14.45 and 25.08  $\mu\text{g/mL}$  PTUFR by 2.66 and 3.24, respectively, fold change as compared before incubation with PTUFR. From Fig. "5B", the gene expressions of p53 in MCF-7 and HepG2 cancer cells were increased post incubation for 48 hours with 14.45 and 25.08  $\mu\text{g/mL}$  PTUFR by 2.45 and 3.11, respectively, fold change as compared before incubation with PTUFR (Anilkumar & Bhanu, 2022).

## CONCLUSION

Poly (thiourea–formaldehyde) resin is synthesized by gamma rays using  $^{60}\text{Co}$  as the main source of irradiation. The characterization techniques are used are FTIR,  $^1\text{H}$ -NMR spectroscopy,  $^{13}\text{C}$ -NMR spectroscopy, TEM and GPC. The poly (thiourea–formaldehyde) resin (PTUFR) is exploited in antimicrobial and cytotoxic activities. The results confirm the formation of PTUFR. The antimicrobial activity of PTUFR is tested against aquatic microbes *Bacillus subtilis* Gram-positive, and *Pseudomonas aeruginosa* negative bacteria and *Candida albicans* fungi that can be used for environmental and medical disinfection. PTUFR has shown bio-applicability to inactivating microbial cells by killing them through interaction with cell membranes and internal cellular components. Reaction with cell wall proteins reduced permeability, whereas high rates of ROS, RNS and RSS release from PTUFR caused damage to DNA and cellular components and ultimately resulted in cell death. Moreover, the cytotoxicity of PTUFR against human breast cancer MCF-7 and HepG2 liver cancer cells was investigated. The cytotoxicity of PTUFR on cancer cell lines resulted in inhibition of cell growth determined by MTT assay. The exposure of MCF-7 and HepG2 cancer cells to PTUFR for 48 hours showed a potential apoptotic activity by significant upregulation of p53 gene expression and cytotoxic activity by downregulation of Bcl-2 gene expression. Therefore, these finding may provide an unconventional strategy for safe wastewater disinfection and as cytotoxic effect as well. Finally, this type of synthesis needs further investigation.

## REFERENCES

- Abel, S.D.A. and Baird, S.K. (2018).** Honey is cytotoxic towards prostate cancer cells but interacts with the MTT reagent: Considerations for the choice of cell viability assay. *Food Chemistry*, 241: 70-78.
- Anilkumar, A. and Bhanu, A.P.A. (2022).** *In vitro* anticancer activity of “Methanolic extract of papaya blackseeds” (MPB) in Hep G2 cell lines and its effect in the regulation of *bcl-2*, *caspase-3* and *p53* gene expression. *Advances in Cancer Biology - Metastasis*, 4: 100025.
- Arafa, W.A.A.; Ghoneim, A.A.; and Mourad, A.K. (2022).** N-Naphthoyl thiourea derivatives: an efficient ultrasonic-assisted synthesis, reaction, and *in vitro* anticancer evaluations. *ACS Omega*, 7(7): 6210–6222.
- Azzam, A.M.; Shenashen, M.A.; Mostafa, B.B.; Kandeel, W.A. and El-Safty, S.A. (2019).** Antibacterial activity of magnesium oxide nanohexagonal sheets for wastewater remediation. *Environmental Progress & Sustainable Energy*, 38(S1): 260-266.
- Azzam, A.M.; Shenashen, M.A.; Selim, M.S.; Mostafa, B.; Tawfik, A. and El-Safty, S.A. (2022).** Vancomycin-loaded ferric amino magnetic nanospheres for rapid detection of gram-positive water bacterial contamination. *Nanomaterials*, 12: 510-524.
- Badr, E.A.; Assar, M.F.; Eltorgoman, A.A.; Labeeb, A.Z.; Breakey, G.A. and Elkhoully E.A. (2020).** A correlation between BCL-2 modifying factor, p53 and livin gene expressions in cancer colon patients. *Biochemistry and Biophysics Reports*, 22: 100747.
- Bai, Z.; Zhou, Q.; Zhu, H.; Ye, X.; Wu, P. and Ma, L. (2021).** QTMP, a novel thiourea polymer, causes DNA damage to exert anticancer activity and overcome multidrug resistance in colorectal cancer cells. *Front. Oncol.*, 11: 667689.
- Barzaga, R.; Lestón-Sánchez, L.; Aguilar-Galindo, F.; Estévez-Hernández, O.; and Díaz-Tendero, S. (2021).** Synergy effects in heavy metal ion chelation with aryl- and aroyl-substituted thiourea derivatives. *Inorg. Chem.*, 60(16): 11984–12000.
- Benis, K.Z.; McPhedran, K.N. and Soltan, J. (2022).** Selenium removal from water using adsorbents: A critical review. *Journal of Hazardous Materials*, 424(C): 127603.
- Chen, L.; Fu, P.; Wang, H.; and Pan, M. (2021).** Excited-state intramolecular proton transfer (ESIPT) for optical sensing in solid state. *Adv. Optical Mater.*, 9(23): 2001952
- Dylağ, M.; Sawicki A. and Ogórek, R. (2019).** Diversity of species and susceptibility phenotypes toward commercially available fungicides of cultivable fungi colonizing bones of *Ursus spelaeus* on display in Niedźwiedzia cave (Kletno, Poland). *Diversity*, 11(12): 224.
- El-Liethy, M.A.; Elwakeel, K.Z. and Ahmed, M.S. (2018).** Comparison study of Ag(I) and Au(III) loaded on magnetic thiourea-formaldehyde as disinfectants

- for water pathogenic microorganism's deactivation. *J. Environ. Chem. Engine.*, 6(4): 4380-4390.
- Ganesan, P.; Staykov, A.; Mufundirwa, A.; Sugiyama, T.; Shu, H.; Uejima M. and Nakashima, N. (2022).** Designing a nickel(II) thiourea-formaldehyde polymer/nanocarbon bifunctional molecular catalyst with superior ORR, OER activities and its application to Zn-air battery. *Mater. Adv.*, 3: 6539-6548.
- Hormati, A.; Shiran, J.A.; Molazadeh, M.; Kaboudin, B. and Ahmadpour, S. (2021).** Synthesis of new thioureas derivatives and evaluation of their efficacy as proliferation inhibitors in MCF-7 breast cancer cells by using <sup>99m</sup>Tc-MIBI radiotracer. *Medicinal Chemistry*, 17(7): 766-778.
- Kanwal, S.; Ali, N.Z.; Hussain, R.; Shah, F.U. and Akhter, Z. (2020).** Polythiourea formaldehyde based anticorrosion marine coatings on type 304 stainless steel. *J. Mater. Res. Technol.*, 9(2): 2146-2153.
- Kavyasri, D.; Sundharesan, M. and Mathew, N. (2022).** Design, synthesis, characterization and insecticidal screening of novel anthranilic diamides comprising acyl thiourea substructure. *Pest Manag. Sci.*, (wileyonlinelibrary.com) DOI 10.1002/ps.7196.
- Lewandowska, A.M.; Rudzki, M.; Rudzki, S.; Lewandowski, T. and Laskowska, B. (2019).** Environmental risk factors for cancer – review paper. *Annals Agri. Environ. Med.*, 26(1): 1-7.
- Li, Q.; Wang, L.; Yu, X. and Xu, L. (2020).** Highly efficient removal of silver nanoparticles by sponge-like hierarchically porous thiourea-formaldehyde resin from water. *Journal of Hazardous Materials*, 400: 123184.
- Li, R.; Cen, B.; Duan, W. and Lin, G. (2022).** Synthesis, antifungal activity and 3D-QSAR study of novel anisaldehyde-derived amide-thiourea compounds. *Advanced Fiber Materials*, 19(4): 202101025.
- Liu, R.; Hou, L.; Yue, G.; Li, H.; Zhang, J.; Liu, J.; Miao, B.; Wang, N.; Bai, J.; Cui, Z.; Liu T. and Zhao Y. (2022).** Progress of fabrication and applications of electrospun hierarchically porous nanofibers. *Advanced Fiber Materials*, 4: 604-630.
- Mane, V.D.; Wahane, N.J. and Gurnule, W.B. (2009).** Copolymer resin. VII. 8-hydroxyquinoline-5-sulfonic acid-thiourea-formaldehyde copolymer resins and their ion-exchange properties. *J. Appl. Polym. Sci.*, 111: 3039-3049.
- Ojogbo, E.; Ward, V. and Mekonnen, T.H. (2020).** Functionalized starch microparticles for contact-active antimicrobial polymer surfaces. *Carbohydrate Polymers*, 229: 115422.
- Sayed, A.R.; Abd El-lateef H.M. and Mohamad, A.D.M. (2018).** Polyhydrazide incorporated with thiadiazole moiety as novel and effective corrosion inhibitor for C-steel in pickling solutions of HCl and H<sub>2</sub>SO<sub>4</sub>. *Macromol. Res.*, 26: 882-891.
- Uçak, Ş.Ş.; & Aydın, A. (2022).** A novel thiourea derivative for preconcentration of copper(II), nickel(II), cadmium(II), lead(II) and iron(II) from seawater samples for Flame Atomic Absorption Spectrophotometry. *Marine Pollution Bulletin*, 180: 113787.

- Wang, J.; Yang, L.; Wang H.; and Wang, L. (2022).** Application of microfluidic chips in the detection of airborne microorganisms. *Micromachines*, 13(10): 1576.
- Ward, Z.J.; Scott, A.M.; Hricak, H. and Atun, R. (2021).** Global costs, health benefits, and economic benefits of scaling up treatment and imaging modalities for survival of 11 cancers: a simulation-based analysis. *The Lancet Oncology*, 22(3): 341-350.
- Xu, Y.; Han, Y.; Li, Y.; Li, J.; Li, J. and Gao, Q. (2022).** Preparation of a strong, mildew-resistant, and flame-retardant biomimetic multifunctional soy protein adhesive via the construction of an organic-inorganic hybrid multiple-bonding structure. *Chem. Engine. J.*, 437(2): 135437.
- Xue, W.; Sewell, C.D.; Zhou, Q.; and Lin, Z. (2022).** Metal–organic frameworks for ion conduction. *Angew. Chem.*, 134(34): 202206512.
- Zhong, Y.; Godwin, P.; Jin, Y. and Xiao, H. (2020).** Biodegradable polymers and green-based antimicrobial packaging materials: A mini-review. *Adv. Ind. Eng. Poly. Res.*, 3(1) 27-35.